Molecular Cancer Therapeutics

Enhanced Antitumor Efficacy of Oncolytic Adenovirus–loaded Menstrual Blood–derived Mesenchymal Stem Cells in Combination with Peripheral Blood Mononuclear Cells

Rafael Moreno[1], Carlos Alberto Fajardo[1], Marti Farrera-Sal[1,2], Ana Judith Perisé-Barrios[3], Alvaro Morales-Molina[3], Ahmed Abdullah Al-Zaher[1], Javier García-Castro[3], and Ramon Alemany[1]

Abstract

Several studies have evaluated the efficacy of using human oncolytic adenovirus (OAdv)–loaded mesenchymal stem cells (MSC) for cancer treatment. For example, we have described the antitumor efficacy of CELYVIR, autologous bone marrow–mesenchymal stem cells infected with the OAdv ICOVIR-5, for treatment of patients with neuroblastoma. Results from this clinical trial point out the role of the immune system in the clinical outcome. In this context, a better understanding of the immunophenotypic changes of human MSCs upon adenoviral infection and how these changes affect human autologous or allogeneic peripheral blood mononuclear cells (PBMC) could guide strategies to improve the antitumor efficacy of infected MSCs. In this work, we show how infection by an OAdv induces toll-like receptor 9 overexpression and activation of the NFB pathway in menstrual blood–derived MSCs, leading to a specific cytokine secretion profile. Moreover, a proinflammatory environment, mainly mediated by monocyte activation that leads to the activation of both T cells and natural killer cells (NK cell), is generated when OAdv-loaded MSCs are cocultured with allogeneic PBMCs. This combination of allogeneic PBMCs and OAdv-loaded MSCs enhances antitumor efficacy both in vitro and in vivo, an effect partially mediated by monocytes and NK cells. Altogether our results demonstrate not only the importance of the immune system for the OAdv-loaded MSCs antitumor efficacy, but in particular the benefits of using allogeneic MSCs for this therapy.

Introduction

Among the variety of strategies designed to improve the limited antitumor efficacy observed after systemic oncolytic adenovirus (OAdv) administration in clinical trials, the use of mesenchymal stem cells (MSC) as cell carriers for OAdv is of special interest because of their natural tumor tropism (1) and immunomodulatory properties (2). In the last decades, we and others have studied the use of MSCs as cell carriers for OAdvs. In this context, CELYVIR, a therapeutic approach exploiting the use of autologous human bone marrow–derived MSCs as cell carriers for the OAdv ICOVIR5, has been evaluated in clinical studies for pediatric refractory metastatic neuroblastoma treatment (NTC01844661). Results from this clinical trial demonstrated tolerance to the treatment and clinical responses including complete remissions (3, 4). The activation status of the immune system of the patients and the inflammatory profile of the MSCs were suggested to play a role in treatment outcome (4). Recently, a dog version of CELYVIR consisting in the combination of dog healthy allogeneic MSCs infected with a canine OAdv has been evaluated in a clinical study to treat spontaneous canine tumor (5). A 74% response rate was determined in the assay with 14.8% showing complete responses, including total remissions of lung metastasis. Interestingly, microenvironment alterations and immune cell infiltration in tumor after treatment were observed. Altogether, these clinical data pointed out the main role of the immune system for OAdv-loaded MSCs antitumor efficacy although more experimental evidences are needed to better understand the immune mechanisms involved in the antitumor efficacy of CELYVIR.

The immunosuppressive properties of MSCs have been extensively reported (2, 6, 7). However, in 2010, the group of Aline Betancourt introduced a new paradigm for MSCs: their polarization into a proinflammatory MSC1 or an immunosuppressive MSC2 phenotype (8, 9), with a clear impact on tumor growth (10). More recently it has been reviewed how pathogen-associated molecular patterns modulate MSCs immunophenotype by signaling through toll-like receptors (TLR), including the activation of TLR-3 by poly(I:C), TLR-4 by lipopolysaccharide, or TLR-9 by non-methylated CpG sequence (11, 12). Recognition of unmethylated CpG motifs from adenovirus double-stranded DNA (ds DNA) by dendritic cells' TLR-9 leads to their maturation and induces transcriptional activation of proinflammatory

[1]Virotherapy and Gene therapy Group, ProCure Program, Translational Research Laboratory, Instituto Catalan de Oncología-IDIBELL, Barcelona, Spain. [2]VCN Biosciences S.L., Grifols Corporate Offices, Sant Cugat del Vallès, Spain. [3]Cellular Biotechnology Unit, Institute of Health Carlos III (ISCIII), Majadahonda, Madrid, Spain.

Note: Supplementary data for this article are available at Molecular Cancer Therapeutics Online (http://mct.aacrjournals.org/).

Corresponding Author: Rafael Moreno, IDIBELLInstituto Catalan de Oncologia-IDIBELL, Gran Via de l'Hospitalet 199, Barcelona 08908, Spain. Phone: 932-607-252; Fax: 932-607-466; E-mail: rafamoreno@iconcologia.net

doi: 10.1158/1535-7163.MCT-18-0431

cytokines and inflammasome components (13). Thus, although it has not been demonstrated for human MSCs, it is plausible to hypothesize that adenoviral infection could switch the immunophenotype of MSCs toward a proinflammatory status through the activation of TLR-9.

Systemic administration of OAdv-loaded MSCs has been used in several animal models (14–18). However, the animal models used to date limit the study of proinflammatory status of MSCs after OAdv infection and its effect on tumor growth. On one hand, immunodeficient mice bearing human xenograft tumors lack a complete immune system and proinflammatory responses. On the other hand, human adenoviruses show species-specific replication, thus limiting the study of oncolysis and antitumor immune responses in immunocompetent mice.

We have recently described the advantages of using menstrual blood–derived MSCs as an alternative to bone marrow–MSCs as cell carriers for OAdv (19). In this follow-up study, we sought to assess the antitumor efficacy of OAdv-infected human menstrual blood–derived MSCs in the presence of autologous and allogeneic human peripheral blood mononuclear cells (PBMC). We show that infection by OAdv induces MSCs immunophenotypic profile changes, generating a proinflammatory environment in cocultures with allogeneic PBMCs, mainly mediated by monocyte activation, and resulting in the activation of both T cells and natural killer cells (NK cell). Finally, we demonstrate that combination of allogeneic PBMCs and OAdv-loaded MSCs present an enhanced antitumor efficacy both *in vitro* and *in vivo*, with monocytes and NK cells playing an important role in this efficacy.

Materials and Methods

Cell culture

The cancer cell lines A549 (human lung adenocarcinoma), A431 (epidermoid carcinoma), FaDu (pharynx squamous cell carcinoma), and HEK-293 (human embryonic kidney) were obtained and authenticated by short tandem repeat profiling by the ATCC. All tumor cell lines were maintained with DMEM supplemented with 5% or 10% FBS and 1% penicillin/streptomycin (Life Technologies) at 37°C, 5% CO_2. Cell lines were routinely tested for *Mycoplasma* presence. The A431-GL and FaDu-GL cell lines were generated by sorting of A431 and FaDu cells previously transduced with a lentiviral vector encoding GFP and luciferase. Isolation and characterization of MSCs has been described previously (19). Although different MSCs passages were used through the different experiments (based on sample availability), the same cell passage from different donors was always used for each experiment, being 5 the highest passage used.

All experiments employing human PBMCs were approved by the ethics committees of the University Hospital of Bellvitge and the Blood and Tissue Bank from Catalonia. PBMCs of healthy donors were isolated from the blood by Ficoll (Rafer) density gradient centrifugation in Leucosep Tubes (Greiner Bio-One) following manufacturer's recommendations. NK- or monocyte-depleted PBMCs were generated using human CD56 or CD14 microbeads, respectively, LD columns, and MidiMACS separator (all from Miltenyi Biotec).

OAdv

The OAdv used throughout this work has been ICOVIR15, previously described by our group (20).

Flow cytometry analysis of TLR-9

MSCs (1×10^5 cells/sample) from three different donors (passage 3) were infected with ICOVIR15 at 50 TU/cell. After 24 hours, cells were analyzed by flow cytometry for expression of TLR-9. Allophycocyanin (APC)-conjugated antibody against TLR-9 (Thermo Fisher Scientific, clone eB72-1665) was used. A Gallios Cytometer (Beckman Coulter) was used and 1×10^4 events were analyzed for each sample. FlowJo v7.6.5 (Tree Star, Inc.) software was used for the analysis of the data.

NFκB reporter luciferase assay

A total of 1×10^5 MSCs (passage 2) were transduced for 16 hours with the nonreplicative lentiviral vector pHAGE-NFB-TA-LUC-UBS-GFP-W (kindly provided by J. García-Castro, Addgene plasmid no. 49343, Institute of Health Carlos III, Majadahonda, Madrid, Spain) at a multiplicity of infection (MOI) of 2. This lentiviral vector encodes the NFκB consensus–binding sequence upstream of the minimal TA promoter of herpes simplex virus followed by the firefly luciferase and GFP genes under the control of the ubiquitin-C promoter. Transduced MSCs were infected with ICOVIR15 at 50 TU/cell, and luciferase activity from cell lysis was determined at different time points postinfection using the Luciferase Assay System (Promega Corporation).

Cytokine array and luminex quantification

A total of 1×10^6 MSCs (passage 3) were infected with ICOVIR15 at 50 TU/cell in duplicate. After 48 hours, the supernatant from infected or uninfected MSCs was collected and the secreted cytokine profile was evaluated using two different analyses: the Proteome Profiler Human Cytokine Array Kit (R&D) and the Th1/Th2/Th9/Th17/Th22/Treg Cytokine 18-Plex Human ProcartaPlex Panel (Thermo Fisher Scientific). For the former, cytokine quantification was determined by estimating the spot integrated density using the ImageLab Software (Bio-Rad Laboratories). For the cytokine array using the multiplexing unit MAGPIX (Luminex Corporation) and the ProcartaPlex Analyst Software (Thermo Fisher Scientific) for the ProcartaPlex Panel.

ELISA

MSCs (2.5×10^5 cells/well in 6-well plaques) from three different donors (passage 3) were infected with ICOVIR15 at an MOI of 50 for 24 hours. The next day, PBMCs from the same donors or from an allogeneic donor were isolated using Ficoll gradient centrifugation. Autologous or allogeneic PBMCs (2.5×10^6 PBMCs) were cocultured with infected or uninfected MSCs (PBMCs:MSCs = 10). After 48 hours of incubation, coculture supernatants were collected and cytokine level was assessed with the human IFNγ, TNFα (PeproTech), IL2 (BioLegend), or IFNα (Mabtech AB) ELISA kits according to the manufacturer's instructions.

Flow cytometry analysis of PBMC activation. For the T and NK cells' activation assay, MSCs from three different donors (passage 4) were infected with ICOVIR15 at a MOI of 50 for 24 hours. The next day, PBMCs from autologous and one allogeneic donor were isolated and cocultured directly in contact or using a transwell system with infected or uninfected MSCs (PBMCs:MSCs ratio of 10) in triplicate. After 48 hours of coculture, PBMCs were harvested, stained for cell viability with LIVE/DEAD Green (Thermo Fisher Scientific), and divided into two different samples followed by incubation with: panel 1 (T-cell activation) and panel 2 (NK

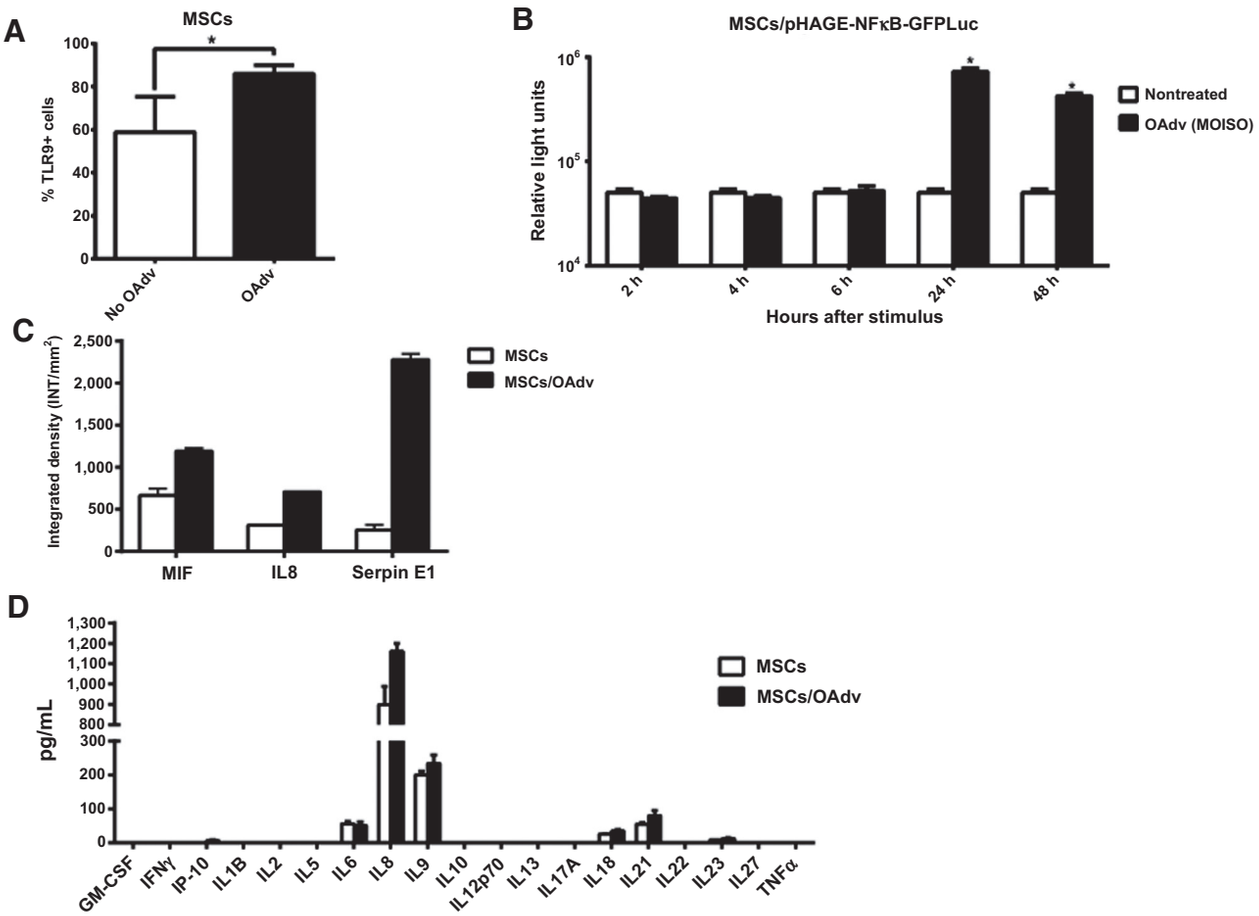

Figure 1.

Effect of OADv infection on MSCs immunophenotypic profile. **A,** MSCs expressing TLR-9 was analyzed by flow cytometry on OAdv-infected (black) or -uninfected (white) MSCs. Bars represent the mean ± SD of triplicates from three independent experiments. *, $P < 0.05$ by Mann–Whitney test. **B,** Luciferase activity was determined from OAdv-infected or -uninfected MSCs/pHAGE-NFκB-GFP/Luc cell lysates at different time-points after infection. Bars represent the mean ± SD of triplicates from three independent experiments. *, $P < 0.05$ by Mann–Whitney test. The supernatants from uninfected or 48 hours OAdv-infected MSCs were analyzed for the presence of secreted cytokines. **C,** Pixel intensity quantification is shown after Proteome Profiler Human Cytokine Array analysis. IL8, interleukin 8; MIF, Macrophage migration inhibitory factor. Bars represent the mean ± SD of spot duplicates from two independent experiments. **D,** Luminex analysis of cytokine concentration is shown. Bars represent the mean ± SD of duplicates from two independent experiments.

cell activation; see supplementary Material and Methods for antibodies details). A Gallios cytometer was used and 2×10^4 live lymphocytes were analyzed for each sample.

In vitro cytotoxicity assay

MSCs (passage 4) were infected with ICOVIR15 at MOI 50 for 24 hours. The next day, PBMCs from an allogeneic donor were isolated using Ficoll gradient centrifugation. Infected or uninfected MSCs, allogeneic PBMCs, and tumoral cells expressing GFP protein (A431-GL or FaDu-GL) were cocultured in 24-well plates at the following cell density (in triplicates): MSCs (infected or uninfected) 2×10^3 cells/cm^2, A431-GL 1×10^4 cells/cm^2, FaDu-GL 5×10^3 cells/cm^2, and allogeneic PBMCS at 10:1 ratio with respect to tumor cells (1×10^5 or 5×10^4 cells/cm^2 when A431-GL or FaDu-GL were present, respectively). After 5 days in coculture, viable GFP-expressing tumoral cells were determined by flow cytometry (negative for LIVE/DEAD and positive for GFP). CountBright absolute counting beads (Thermo Fisher Scientific) were used for absolute cell number determination. Cytotoxicity was expressed as the percentage of live cancer cells in cocultures normalized to that of cancer cells cultured alone.

In vivo OAdv tumor delivery and antitumor efficacy

In vivo studies were performed at the ICO-IDIBELL Animal Facility (Barcelona, Spain) AAALAC unit 1155, and approved by IDIBELL's Ethical Committee for Animal Experimentation.

Athymic nu/nu mice

Lung adenocarcinoma xenograft tumors were established by implanting 5×10^6 A549 cells subcutaneously into both flanks of 8-week-old female Athymic nu/nu mice. When tumors reached 100–120 mm^3, mice were randomized and distributed into groups. To evaluate systemic efficacy, animals were treated with a single intraperitoneal dose of PBS or 5×10^{10} vp/mice of OAdv (ICOVIR15), MSCs (4×10^6 cells) or MSC/OAdv (4×10^6 cells previously infected with ICOVIR15 at MOI 50 for 24 hours).

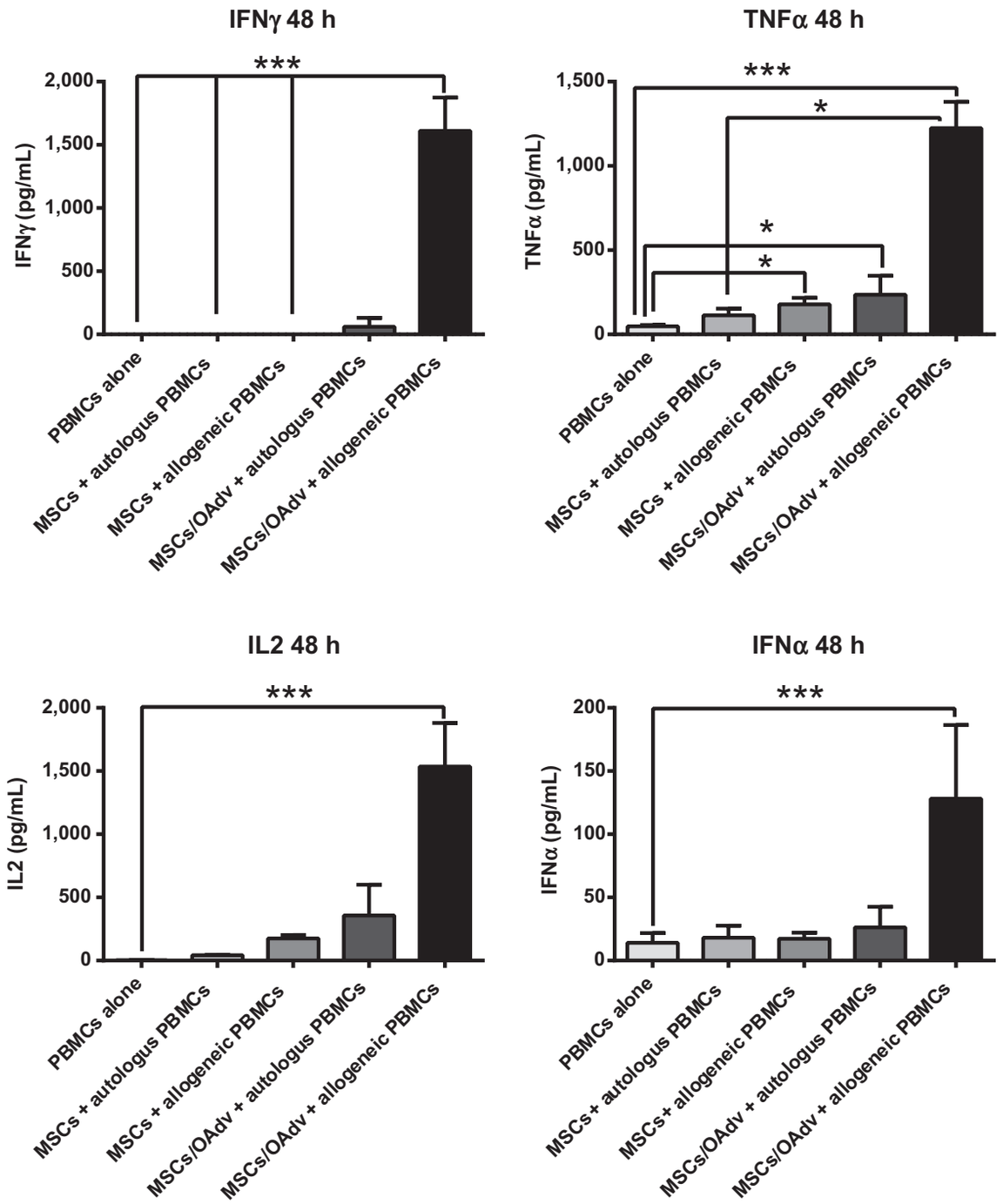

Figure 2.

Proinflammatory cytokines production in autologous or allogeneic PBMCs cocultures with OAdv-infected MSCs. Uninfected or OAdv-infected (MOI = 50) MSCs from three different donors were cocultured with autologous or allogeneic human PBMCs at a PBMCs-to-MSCs ratio of 10 in triplicates. After 48 hours of coculture, culture medium was collected and cytokines level assessed by ELISA. The mean ± SD of triplicates from two independent experiments is shown (*, $P < 0.05$; ***, $P < 0.001$ by Kruskal–Wallis with Dunn *post hoc* test).

NOD/SCID gamma mice

The same tumor model was established, but in this case implanting 5×10^6 A549 or A431 cells suspended in a 100-μL PBS and Matrigel mixture (1:1, volume/volume; BD biosciences) into both flanks of 8-week-old NOD/SCID gamma (NSG) mice. When tumors reached 100–120 mm^3, mice were randomized

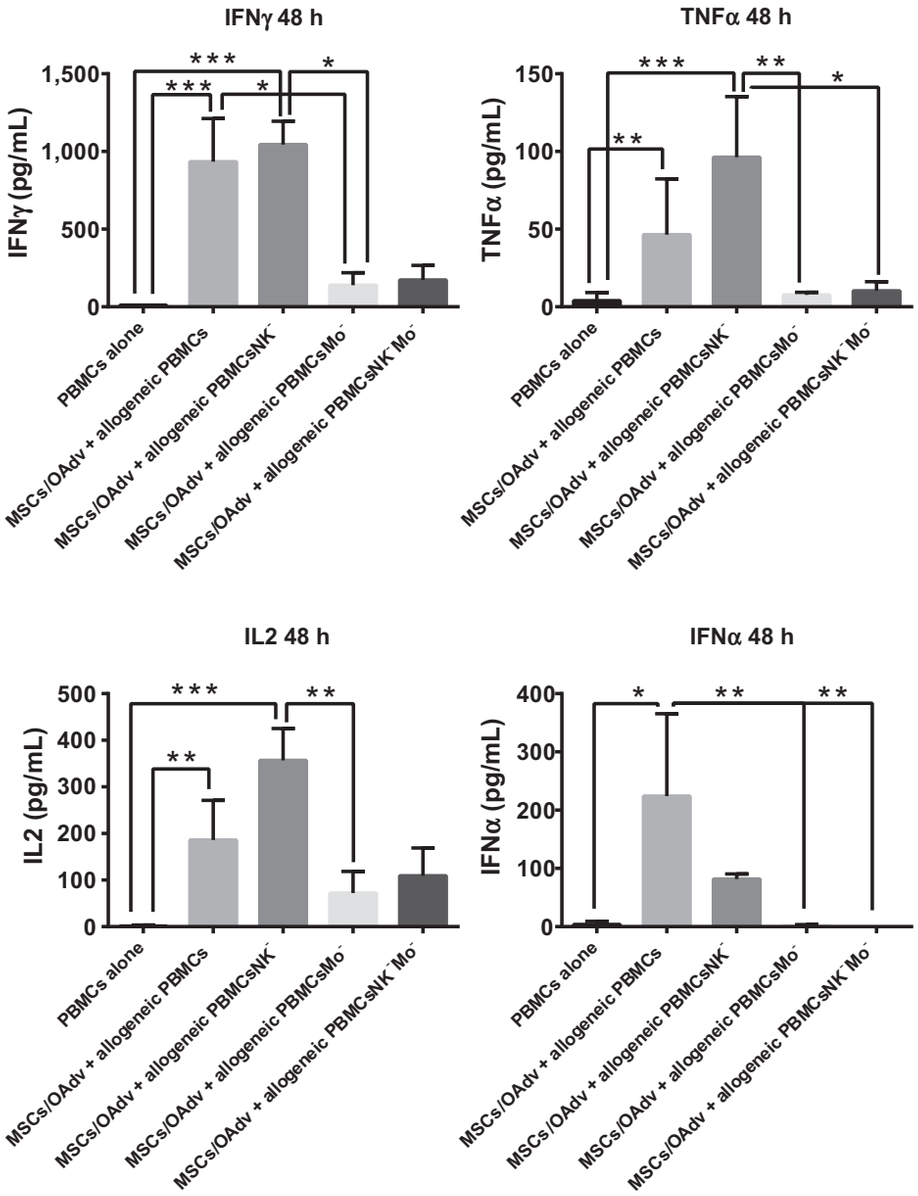

Figure 3.
Effect of monocyte and/or NK-cell depletion on proinflammatory cytokines production in cocultures of OAdv-MSCs and allogeneic PBMCs. Allogeneic human PBMCs from the same donor were depleted for monocytes and/or NK cells, and cocultured with uninfected or OAdv-infected MSCs (PBMCs: MSC = 10). Nondepleted PBMCs alone or in coculture with OAdv-infected MSCs were used as control. After 48 hours of coculture, culture medium was collected and cytokines level assessed by ELISA. The mean ± SD of triplicates from two independent experiments is shown (*, $P < 0.05$; **, $P < 0.01$; ***, $P < 0.001$ by Kruskal–Wallis with Dunn *post hoc* test).

and distributed into the following groups: allogeneic PBMCs + PBS; MSCs; OAdv or MSCs/OAdv (MSCs previously infected with ICOVIR15 at MOI 50 for 24 hours), and MSCs/OAdv without allogeneic PBMCs (only for the A549 experiment). To evaluate antitumor efficacy, 1×10^7 human allogeneic PBMCs were administered to the mice by intravenous injection except animals receiving only MSCs/OAdv. The next day, animals were treated with a single intraperitoneal dose of PBS, 1×10^{10} vp/mice of OAdv (ICOVIR15), 5×10^6 MSCs, or 5×10^6 MSCs/OAdv.

Tumor volume was calculated according to the equation $V\ (\text{mm}^3) = \pi/6 \times W^2 \times L$, where W and L are the width and the length of the tumor, respectively. Data are expressed as the tumor size relative to the size at the beginning of the therapy (tumor growth). At the end of the study, animals were euthanized and tumors were collected. One half was frozen for DNA extraction, and the other half was fixed in 4% formaldehyde for 24 hours and embedded in paraffin.

For the antitumor efficacy studies involving monocytes- and NK-cell–depleted allogeneic PBMCs, the same animal and tumor model were used. When A549 tumors reached 100–120 mm^3, mice were randomized and distributed into the following groups: allogeneic PBMCs + PBS or MSCs/OAdv, allogeneic PBMCs depleted for monocytes + MSCs/OAdv, and allogeneic PBMCs depleted for NK cells + MSCs/OAdv. PBMCs from a single donor were isolated, and a part of the sample was depleted for monocytes or NK cells as described above. Monocytes and NK-cell depletion was confirmed by flow cytometry after staining of the cells with LIVE/DEAD violet, and APC-CD14 or PE-CD56. Finally, 1×10^7 human allogeneic PBMCs, human allogeneic monocytes-depleted PBMCs, or human allogeneic NK cell–depleted PBMCs were

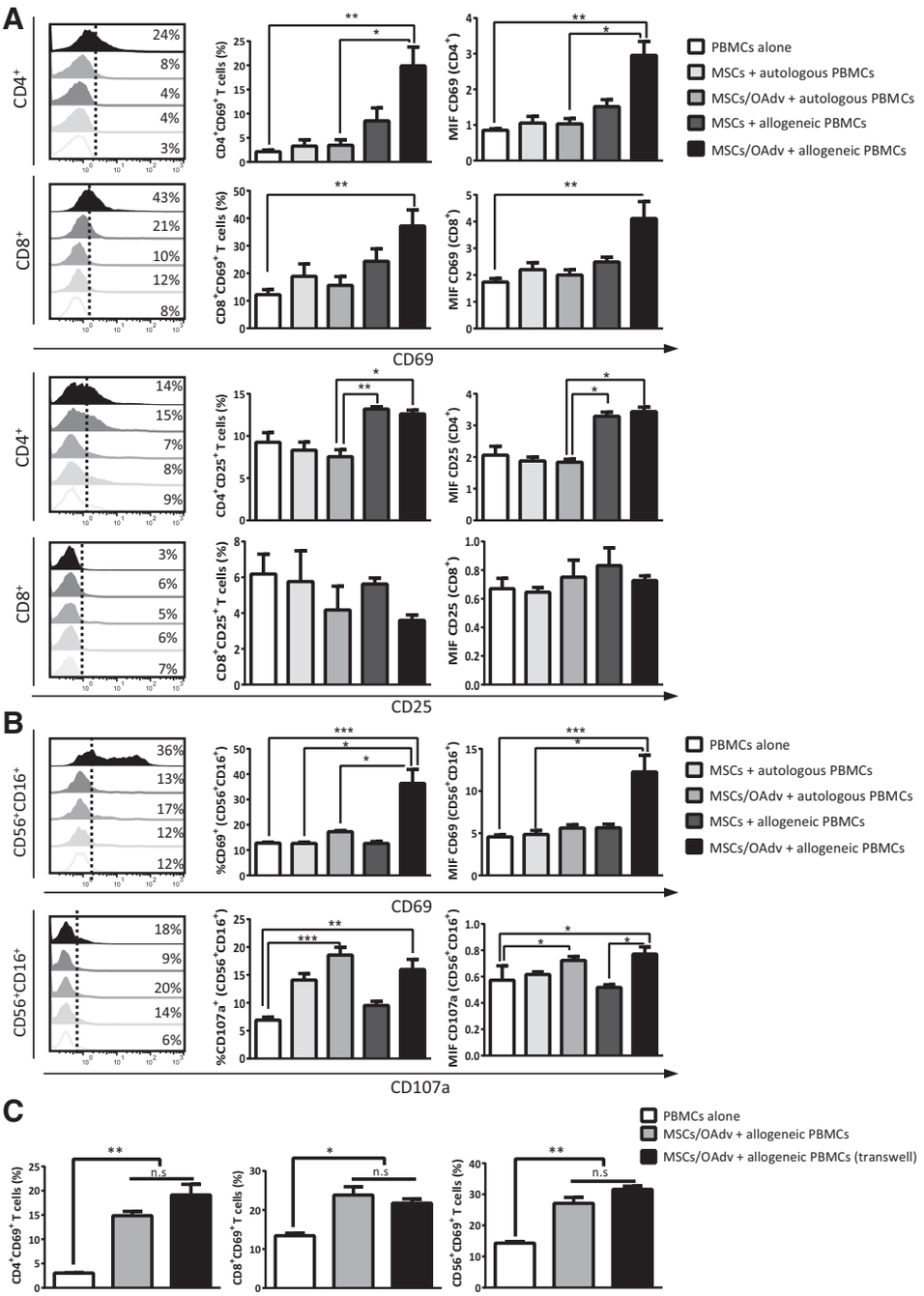

Figure 4.

$CD4^+$ $CD8^+$ T-cell and NK cell activation in cocultures of autologous or allogeneic human PBMCs with OAdv-infected MSCs. Uninfected or OAdv-infected MSCs were cocultured with autologous or allogeneic human PBMCs at a PBMCs-to-MSCs ratio of 10 in triplicates. After 48 hours of coculture, PBMCs were harvested and T cells and NK cells analyzed. **A,** Top, analysis of CD69 expression. Left, example of $CD4^+$- and $CD8^+$-positive cells expressing CD69 histograms in different coculture conditions. Middle, percentage of $CD4^+$- and $CD8^+$-positive cells expressing CD69. Right, CD69 mean fluorescent intensity of $CD4^+$- and $CD8^+$-positive cells. Bottom, analysis of CD25 expression. Left, example of $CD4^+$- and $CD8^+$-positive cells expressing CD25 histograms in different coculture conditions. Middle, percentage of $CD4^+$ (left) and $CD8^+$ (right)-positive cells expressing CD25. Right, CD25 mean fluorescent intensity of $CD4^+$- and $CD8^+$-positive cells. **B,** Top, analysis of CD69 expression. Left, example of $CD56^+CD16^+$-positive cells expressing CD69 histograms in different coculture conditions. Middle, percentage of $CD56^+CD16^+$-positive cells expressing CD69. Right, CD69 mean fluorescent intensity of $CD56^+CD16^+$-positive cells. Bottom, analysis of CD107a expression. Left, example of $CD56^+CD16^+$-positive cells expressing CD107a histograms in different coculture conditions. Middle, percentage of $CD56^+CD16^+$-positive cells expressing CD107a. Right, CD107a mean fluorescent intensity of $CD56^+CD16^+$-positive cells. **C,** Same experiment was performed allowing direct cell contact or using transwells system to separate OAdv-MSCs from allogeneic PBMCs. The percentage of $CD4^+$, $CD8^+$, or $CD56^+CD16^+$-positive cells expressing CD69 is represented. The mean ± SD of triplicates from two independent experiments is shown in all analysis (*, $P < 0.05$; **, $P < 0.01$; ***, $P < 0.001$ by Kruskal–Wallis with Dunn *post hoc* test).

administered to the mice by intravenous injection. Next day, animals were treated with a single intraperitoneal dose of PBS or 5×10^6 MSCs/OAd and tumor size was monitored as described previously.

Determination of adenoviral genomes in tumor samples

A549 frozen tumor samples were mechanically homogenized and total DNA was extracted following the QIAamp DNA Mini Kit (Qiagen) protocol for tissue DNA purification. Adenoviral genome copies were quantified in triplicate by qRT-PCR using the specific set of primers targeting the hexon sequence (forward 5′-CTT CGA TGA TGC CGC AGT G-3′, reverse 5′-ATG AAC CGC AGC GTC AAA CG-3′). PCR conditions were: 95°C 10 minutes, 40 × cycles of 95°C 15 seconds, 60°C 1 minute, and 72°C 7 seconds. Real-time PCR was performed using LightCycler 480 SYBR Green I Master (Roche). Adenoviral genome copy numbers were calculated using a standard curve of serially diluted pAd5wt, a plasmid containing the complete Adenoviral type 5 genome and for which the genome copy number was known.

Histology and IHC

A549 paraffin-embedded sections (5-μm thickness) of tumors samples were treated with an anti-Ad2/5E1A antibody (SC-430, Santa Cruz Biotechnology) as primary antibody diluted 1/200 in PBS. IHC staining was performed with EnVision (Dako), according to manufacturer's instructions, and with hematoxylin and eosin. Images were acquired using the Nikon Eclipse 80i microscope running NIS elements BR software (Nikon Instruments Europe BV).

Statistical analysis

Statistical comparisons between two groups were performed using the Mann–Whitney U test (two-tailed). For comparison of more than two groups, Kruskal–Wallis with Dunn *post hoc* test was used. Statistical significance was established as $P < 0.05$. Data are presented as the mean ± SD or SEM. All statistical analyses were calculated with GraphPad Prism software.

Results

Immunophenotypic profile changes in MSCs after OAdv infection

Adenoviral infection has been described as triggering the expression of TLR-9 in different cell types (21, 22). We therefore decided to evaluate the expression of TLR-9 on MSCs in response to OAdv infection. Twenty-four hours after OAdv infection, the percentage of MSCs-expressing TLR-9 was significantly increased 1.46-fold (Fig. 1A). We next studied the activation of NFκB pathway in MSCs after OAdv infection. For this, MSCs were transduced with a lentiviral vector containing a NFκB promoter–driven luciferase reporter system for detecting NFκB activation (23), and luciferase expression was evaluated at different time points after OAdv infection. Significant expression of luciferase was observed 24 hours postinfection (Fig. 1B), indicating an activation of the NFκB pathway after OAdv infection.

To determine whether OAdv-induced NFκB activation triggers the expression of immune response genes, we evaluated the production of several proinflammatory and immune-related cytokines in uninfected or OAdv-infected MSCs after 48 hours of infection using both, a cytokine array and a Luminex assay. From the 36 cytokines quantified in the cytokine array (Supplementary Fig. S1), only macrophage migration inhibitory factor (MIF), IL8, and Serpin E1could be detected, and all three were overexpressed after OAd infection (fold-increase of 1.79, 2.27, and 9.01, respectively; Fig. 1C). Results from the 19 cytokines evaluated with the Luminex assay confirmed the overexpression of IL8 (fold-increase of 1.29), and revealed a slight increase in the expression of IL9, IL18, and IL21 after virus infection (Fig. 1D).

By knocking down the TLR-9 expression on MSCs using a lentivirus coding for a short hairpin RNA against the human TLR-9, we confirmed the role of the receptor on the NFκB pathway activation and cytokines expression after OAdv infection (Supplementary Fig. S2).

In summary, these results indicate an increase in the secretion profile of specific proinflammatory cytokines in response to the

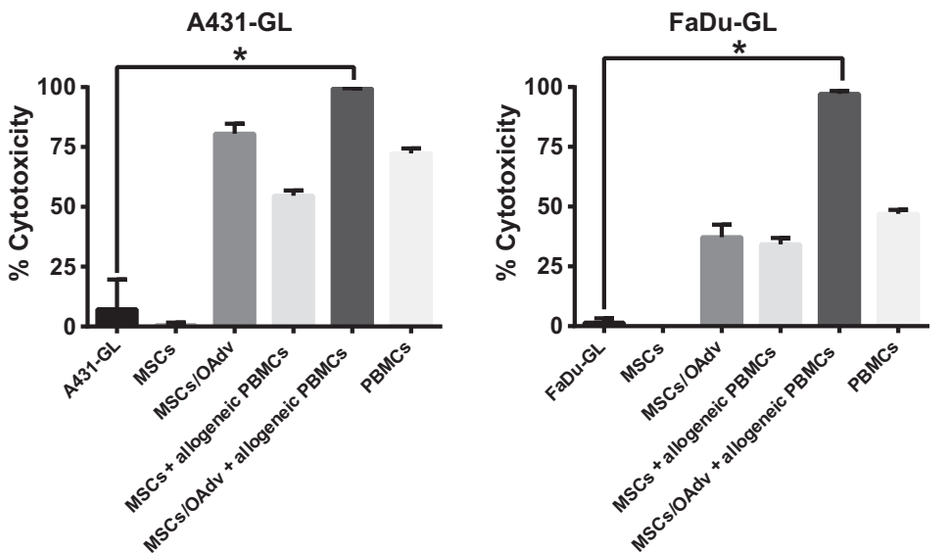

Figure 5.
Antitumor efficacy of OAdv-loaded MSCs *in vitro*. A431-GL and FaDu-GL cancer cell lines were cocultured with OAdv-infected or -uninfected MSCs in the presence or absence of allogeneic PBMCs (PBMCs:cancer cell ratio = 10) in triplicates. After 5 days in coculture, live cancer cells were counted by flow cytometer. Cytotoxicity was expressed as the percentage of live cancer cells on cocultures, normalized to the number of cancer cells cultured alone (*, $P < 0.05$ by Kruskal–Wallis with Dunn *post hoc* test). Results from two independent experiments are shown.

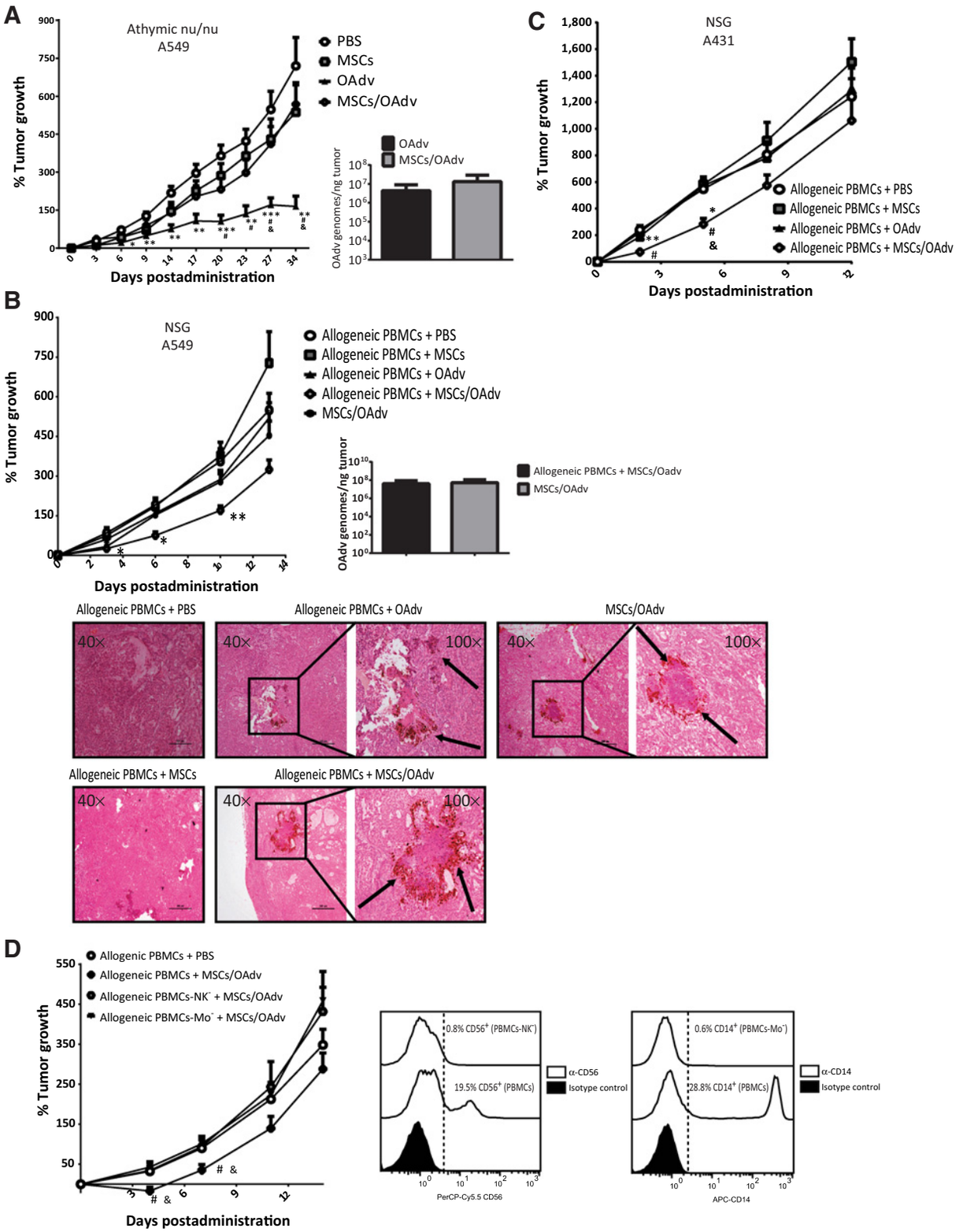

Figure 6.

Antitumor efficacy of OAdv-loaded MSCs *in vivo*. **A,** Athymic nu/nu mice bearing subcutaneous A549 tumors were intraperitoneally injected with PBS, MSCs, OAdv, or MSCs previously infected with OAdv ($n = 7$ mice per group). Left, the mean of tumor growth ± SEM is shown. (*Continued on the following page.*)

NFκB pathway activation in MSCs after OAdv infection, as a result the activation of TLR-9 by viral genome.

OAdv-infected MSCs stimulate a proinflammatory environment in coculture with allogeneic PBMCs. To evaluate whether OAdv-loaded MSCs have an effect on the immunologic status of PBMCs, we first analyzed the expression of several proinflammatory cytokines from autologous or allogeneic human PBMCs cocultured with uninfected or OAdv-infected MSCs for 48 hours. Uninfected MSCs, independently from the source of the PBMCs, and infected MSCs in coculture with autologous PBMCs had no significant effect on the secretion of cytokines by PBMCs (Fig. 2). However, a significant increase in the expression level of all four cytokines evaluated was observed when human allogeneic PBMCs were cocultured in the presence of OAd-infected MSCs, indicating the induction of a proinflammatory environment in the coculture. To determine the contribution of different cell subtypes in the induction of this proinflammatory environment, infected or uninfected MSCs were cultured in the presence of allogeneic PBMCs from which monocytes, NK cells, or both were previously depleted. We found that the depletion of monocytes in the coculture significantly decreased the level of all four cytokines indicating their importance in establishing the proinflammatory environment (Fig. 3).

To evaluate whether this proinflammatory environment triggers the activation of the different cell subtypes in PBMCs, we further investigated the activation of autologous and allogeneic $CD4^+$ T cells, $CD8^+$ T cells, and NK cells in coculture with infected or uninfected MSCs. As shown in Fig. 4A, proinflammatory cytokines secreted by the coculture of human allogeneic PBMCs and OAd-infected MSCs induced $CD8^+$ and $CD4^+$ T-cell activation as indicated by an increase in the expression of the activation markers CD69 in both cell lines, and CD25 in $CD4^+$ T cells in response not only to the presence of the virus but also in the use of allogeneic PBMCs. Similarly, the percentage and intensity of NK cells ($CD56^+CD16^+$) expressing the activation marker CD69 was significantly higher when allogeneic PBMCs were cocultured with OAd-infected MSCs (Fig. 4B). Moreover, the percentage and intensity of NK cells expressing the degranulation marker CD107a was significantly higher when OAd-infected MSCs were cocultured not only with allogeneic but also with autologous PBMCs, probably indicating the effect of the OAdv on NK cell activation. To confirm that secreted factors from OAdv-infected MSCs induce the observed T-cells and NK-cell activation, a similar experiment was carried out but including a transwell assay to separate PBMCs from infected MSCs. Thus, CD69 upregulation was measured and compared on $CD8^+$, $CD4^+$, or $CD56^+CD16^+$cells employing direct contact cell-to-cell or transwell coculture assays. As shown in Fig. 4C, whereas a similar and significant CD69 upregulation was detected for all cell types evaluated independently of the coculture conditions (direct cell-to-cell contact or using transwells), no differences where determined between the coculture methodology used. This result points out the role of the soluble factor secreted by OAdv-secreted MSCs on cell activation.

Overall these finding demonstrate that coculture of allogeneic PBMCs and OAdv-loaded MSCs induce a proinflammatory environment mediated in part by monocytes, which results in the activation of $CD8^+$, $CD4^+$ T cell, and NK cells.

Allogeneic PBMCs enhance the antitumor efficacy of OAdv-loaded MSCs in vitro. We next addressed whether allogeneic PBMCs could increase the antitumor efficacy of OAdv-infected MSCs *in vitro*. For this, two different GFP-expressing cancer cell lines (A431-GL and FaDu-GL, both of them considered partly resistant to adenovirus infection) were cocultured with OAdv-infected or -uninfected MSCs in the presence or absence of allogeneic PBMCs for 5 days, and the percentage of cancer cell death was determined by flow cytometry. The combination of allogeneic PBMCs and OAdv-loaded MSCs showed increased antitumor efficacy compared with OAdv-infected MSCs alone or uninfected MSCs in combination with allogeneic PBMCs (Fig. 5).

Allogeneic human PBMCs increase the antitumor efficacy of OAdv-loaded MSCs *in vivo*

We recently reported the tumor homing properties of MSCs/OAdv after systemic administration in human tumor–bearing athymic nu/nu mice (19), but the antitumor efficacy of this strategy was not evaluated. We therefore evaluated the antitumor efficacy of OAdv-loaded MSCs in A549-tumor bearing nude mice. In contrast to the treatment with OAdv alone, in which tumor growth was significantly controlled, OAdv-loaded MSCs showed only moderate antitumor efficacy (Fig. 6A). These results suggest that although MSCs migrated to the tumors after systemic administration, the amount of cells arriving at and the number of virus particles delivered to the tumors during the first days after treatment was not enough to control tumor growth. Nevertheless, the total viral genomes detected in tumors at the end of the experiment were similar to the OAdv group. This apparently contradiction could be explained considering that the OAdv content in tumor at early stages of the experiment determines the antitumor efficacy at later stages. Thus, directly administrated OAdv leads to a larger amount of initial virus in the tumor that is able to control

(*Continued.*) *, $P < 0.05$; **, $P < 0.01$; ***, $P < 0.001$ OAdv versus PBS group; #, $P < 0.05$ OAdv versus MSCs; &, $P < 0.05$ OAdv versus MSCs/OAdv group by Kruskal–Wallis with Dunn *post hoc* test. Right, the presence of OAdv genomes in tumors at the end of the experiment was assessed by real-time PCR. **B,** NSG mice bearing subcutaneous A549 tumors received an intravenous injection of human allogeneic PBMCs except one group ($n = 7$ mice per group). Next day, mice were intraperitoneally injected with PBS, MSCs, OAdv, or MSCs previously infected with OAdv. Left, the mean of tumor growth ± SEM is shown. *, $P < 0.05$; **, $P < 0.01$ allogeneic PBMCs + MSC/OAdv versus PBS group by Kruskal–Wallis with Dunn *post hoc* test. Right, the presence of OAdv genomes in tumors at the end of the experiment was assessed by real-time PCR. Bottom, IHC staining of E1A of a representative tumor from each group is shown. The arrow points to positive virus E1A staining. **C,** NSG mice bearing subcutaneous A431 tumors were treated as described previously. The mean of tumor growth ± SEM is shown. *, $P < 0.05$; **, $P < 0.01$ allogeneic PBMCs + MSC/OAdv versus PBS group; #, $P < 0.05$ allogeneic PBMCs + MSC/OAdv versus MSCs; &, $P < 0.05$, allogeneic PBMCs + MSC/OAdv versus OAdv group, by Kruskal–Wallis with Dunn *post hoc* test. **D,** NSG mice bearing subcutaneous A549 tumors received an intravenous injection of human allogeneic PBMCs or PBMCs previously depleted for monocytes or NK cells ($n = 7$ mice per group). Next day, mice were intraperitoneally injected with PBS, or MSCs previously infected with OAdv. Right, the mean of tumor growth ± SEM is shown (#, $P < 0.05$, allogeneic PBMCs + MSC/OAdv vs. allogeneic PBMCs-NK^- + MSC/OAdv group; &, $P < 0.05$, allogeneic PBMCs + MSC/OAdv vs. allogeneic PBMCs-Mo^- + MSC/OAdv group by Kruskal–Wallis with Dunn *post hoc* test). Left, analysis of the percentage of $CD56^+$ cells and $CD14^+$ cells in PBMC and NK- or monocytes-depleted PBMCs samples, respectively.

tumor growth but also depletes the substrate (tumor cells) faster. Tumors develop fibroblast barriers, which do not allow the efficient spread of the virus, and these barriers form isolated tumor nodules that eventually grow without virus. At the end of the experiments the tumors analyzed contained few virus despite their lower size. However, for the MSCs/OAdv group, because the initial amount of virus in the tumor is lower, the scarce amount of foci of replicating virus cannot eliminate all the tumor cells in these fast-growing tumor models and there is no apparent antitumor efficacy but as the permissive substrate (tumor cells) is not eliminated, the virus is amplified progressively until the end of the experiment.

Because the above described *in vitro* characterization strongly suggests an important role of MSC/OAdv in modulating the antitumor immune response of allogeneic PBMCs, we hypothesized that the *in vivo* antitumor efficacy of MSC/OAdv could be improved in the presence of human immune cells. We decided to use the immunodeficient mouse model NSG with human tumors and human PBMCs, a model previously used to evaluate the combination of human adenovirus and human PBMCs (24, 25).

Thus, NSG mice bearing subcutaneous A549 tumors received an intravenous injection of 10^7 human allogeneic PBMCs. The next day, mice received a single intraperitoneal injection of PBS, OAdv (ICOVIR15), MSCs, or MSC/OAdv. A group consisting of mice treated with MSC/OAdv in the absence of human allogeneic PBMCs was also included to specifically evaluate the effect of the human allogeneic PBMCs on the MSC/OAdv antitumor activity. To simplify the experiment, and taking into account our previous result where human PBMCs had no effect on tumor growth (24), we did not evaluate the rest of the groups in the absence of human PBMCs. As shown in Fig. 6B, antitumor efficacy could be detected only when OAdv-loaded MSCs were combined with the administration of allogeneic PBMCs, pointing out the relevance of allogeneic PBMCs in the antitumor effect. Importantly, there were no differences in the viral load in the tumors at the end of the experiment among MSCs OAdv-loaded groups in the presence or absence of human allogeneic PBMCs, indicating that PBMCs did not interfere with MSCs/OAdv tumor–homing. A visual not quantitative analysis of diverse IHC images from each group was performed to confirm the presence of OAdv in the tumors. Histology of the tumors at the end of the experiment revealed the expression of the E1a protein in tumors of animals treated with the OAdv alone or in combination with MSCs, confirming the correct OAdv delivery and amplification in tumors. We also tested the antitumor efficacy of the different groups in the presence of human allogeneic PBMCs in a second tumor model, NSG mice bearing subcutaneously A431 tumors and transferred with human PBMCs. As shown in the Fig. 6C, a significant tumor growth control was observed only for the MSCs/OAdv-treated group, although it was restricted to early days after treatment (from day 3 to day 8). However, this result is of special interest because A431 are partly resistant to adenovirus infection strongly suggesting the effect of the allogeneic PBMCs on the efficacy observed because low or no viral replication is expected in these tumoral cells.

Effect of monocytes or NK cells' depletion on antitumor activity of OAdv-loaded MSCs *in vivo*

Finally, having demonstrated the importance of monocytes in establishing the proinflammatory environment, and the NK-cell activation *in vitro* after allogeneic PBMCs and OAdv-loaded MSCs coculture, we next evaluated the influence of these cell types on the antitumor efficacy observed *in vivo*. NSG mice bearing subcutaneous A549 tumors received an intravenous injection of 10^7 human allogeneic PBMCs, 10^7 monocyte-depleted human allogeneic PBMCs (PBMCs-Mo$^-$), or 10^7 NK-depleted human allogeneic PBMCs (PBMCs-NK$^-$). Twenty-four hours later, mice received a single intraperitoneally administration of PBS or 5×10^6 MSCs/OAdv. As show in the Fig. 6D, a significant tumor growth control was observed only when a complete PBMCs administration was done. These differences were significant against both; the monocyte- and NK cell–depleted groups, although it was restricted to early days after treatment (from day 3 to day 8). Nevertheless, at the end of the experiment the group transferred with fully PBMCs showed 1.5 and 1.6-fold decrease ($P = 0.066$ and 0.057) in the percentage of tumor growth compared with groups depleted for NK cells and monocytes, respectively. We consider that these results support the hypothesis of the role of the innate response on the tumor control efficacy observed for OAdv-loaded MSCs treatment.

Discussion

In this study we evaluated the effect of OAdv infection on MSCs at the level of their immune profile, their behavior in the presence of autologous or allogeneic human PBMCs, and their impact in antitumor efficacy *in vitro* and *in vivo*. We show that adenovirus infection of MSCs increases the expression of TLR-9, leading to NFκB pathway activation. We also detected an increase in the expression of diverse proinflammatory cytokines, including macrophage MIF, an upstream activator of innate immunity (26), IL8, a proinflammatory cytokine also overexpressed in MSCs after TLR-3 and TLR-4 stimulation (27), and Serpin E1, which stimulates macrophage activation through TLR signaling (28), among others. These results are in agreement with studies evaluating adenovirus infection of dendritic cells showing that, during endosomal trafficking, Ad5 virions are accumulated in the late endosomal compartment where they are fused with vesicles carrying TLR-9 (22). This receptor recognizes unmethylated CpG motifs in the adenovirus dsDNA, leading to transcriptional activation of proinflammatory cytokine and inflammasome-related genes via NFκB and AP-1 signaling pathways (29, 30). Moreover, taking into account the multiple mechanisms used by MSCs to modulate the immune system, we cannot discard additional immunophenotypic changes on MSCs after OAdv infection than those evaluated in this work. Altogether our results confirm that adenovirus infection alters the immune status of MSCs towards a more proinflammatory profile, as a result of OAd-mediated stimulation of TLR-9, as described for other MSCs' TLR stimulation (9).

We further evaluated the effect of this adenovirus-specific MSCs immune profile on the activation of the immune system *in vitro*. A clear proinflammatory environment was detected when infected MSCs were cocultured with allogeneic, but not with autologous, PBMCs. Proinflammatory cytokines were highly expressed (IFNγ, TNFα, IL2, and IFNα) in these coculture conditions, mainly mediated by monocyte activation and probably in response to the presence of adenovirus as described previously (31, 32). Interestingly, this proinflammatory environment was, in part, independent of cell contact but related to soluble factors secreted by infected MSCs. Moreover, this proinflammatory environment led to CD8$^+$ and CD4$^+$ T-cell activation as indicated by an

increase in the expression of CD69 and CD25, in response not only to the presence of the virus but also to the HLA mismatch between the $CD4^+$ T cell and MSCs. Different studies have recently pointed out the capacity of oncolytic virotherapy to promote intratumoral T-cell infiltration and enhance checkpoint inhibitor immunotherapy (33, 34), therefore it is plausible to expect a similar effect for OAdv-infected MSCs. NK-cell activation was also detected when infected MSCs were cocultured with allogeneic PBMCs as shown by the expression of CD69 and CD107a. These results are in agreement with a previous study in which oncolytic reovirus infection stimulate monocytes to secrete IFNα, resulting in NK-cell activation and improved antitumor efficacy (35).

A greater antitumor potency of OAd-loaded MSCs and allogeneic PBMCs combination was confirmed not only *in vitro* (evaluated in FaDu and A431cell lines, partly resistant to adenovirus infection; refs.36, 37), but most importantly *in vivo*. In this work, we demonstrate for the first time the antitumor efficacy of OAdv-loaded MSCs after only a single systemic administration, indicating that this antitumor efficacy is mediated by the presence of allogeneic PBMCs. Moreover, when NK cells are depleted from PBMCs transferred to mice, antitumor efficacy is lost, indicating the important role of NK cells in the antitumor efficacy exerted by OAdv-loaded MSCs. A similar lack of antitumor efficacy was observed with monocyte-depleted PBMCs as expected according to the role described for monocytes on NK cell activation (38, 39) and our own *in vitro* results. Finally, it is worth mentioning the limitation of our model in which only innate immune responses can be studied because no adaptive responses are generated in this mouse model. Thus, this model is likely underestimating the overall antitumor efficacy because recent evidence suggests that NK cells can act as initiators of adaptive immune response (reviewed in ref. 40).

In summary, our work describes the immune-stimulatory properties of allogeneic MSCs infected with OAdvs and their potential benefits as an alternative to the conventional autologous MSCs used in the CELYVIR clinical trials. In this regard, the clinical benefits using OAdv-infected allogeneic MSCs to treat canine tumors also support the use of healthy allogeneic donor MSCs instead of autologous MSCs (5). Interestingly, in this study there was no correlation between the gender of the MSCs donor or patient and the efficacy observed, indicating that OAdv-loaded MSCs could be a potential treatment not only for female but also for male patients. Thus, to create a homogenous and well characterized allogeneic MSCs master bank from allogeneic healthy donors should be considered for the future development of CELYVIR. MenSCs have been extensively characterized *in vitro* and *in vivo*, and their potential for cellular therapy has been described previously (41–43), pointing out that menstrual blood represents an efficient and ethically accepted source of MSCs, and could be considered to generate this MSCs master bank. Finally, data accumulated from patients, dogs, and preclinical assays (including this work) strongly suggest the role of the immune system status in the outcome of the therapy. Although a specific predictive marker has still not been found, assessing the patient immune system and the capability of OAd-loaded MSCs from different donors to activate patients PBMCs could serve as a biomarker for therapy outcome.

From here on, another important factor in improving the efficacy of CELYVIR should be the optimization of the OAdv used by, for example, using more potent OAdvs (44) or OAdvs encoding immunostimulatory sequences or transgenes to enhance the immune response against the tumor (24, 45, 46).

Disclosure of Potential Conflicts of Interest

M. Farrera-Sal is an employee (R&D Department) at VCN Biosciences S.L. No potential conflicts of interest were disclosed by the other authors.

Authors' Contributions

Conception and design: R. Moreno, C.A. Fajardo, R. Alemany
Development of methodology: R. Moreno, C.A. Fajardo, A.J. Perisé-Barrios, A.A. Al-Zaher, J. García-Castro
Acquisition of data (provided animals, acquired and managed patients, provided facilities, etc.): R. Moreno, M. Farrera-Sal, A.J. Perisé-Barrios, A. Morales-Molina, A.A. Al-Zaher, J. García-Castro, R. Alemany
Analysis and interpretation of data (e.g., statistical analysis, biostatistics, computational analysis): R. Moreno, C.A. Fajardo, M. Farrera-Sal, A. Morales-Molina, J. García-Castro, R. Alemany
Writing, review, and/or revision of the manuscript: R. Moreno, C.A. Fajardo, A. Morales-Molina, A.A. Al-Zaher, R. Alemany
Administrative, technical, or material support (i.e., reporting or organizing data, constructing databases): R. Moreno
Study supervision: R. Moreno, R. Alemany

Acknowledgments

The authors thank Jana de Sostoa, Dolores Ramos, and Silvia Torres for their lab technical support. We also thank Vanessa Cervera for samples processing. We are grateful to Ashleigh Jones for grammatical and style proofreading. This work was supported by Asociación Española Contra el Cáncer (AECC), BIO2014-57716-C2-1-R grant (to R. Alemany) and PI14CIII/00005 and PI17CIII/00013 (to J. García-Castro) from the Ministerio de Economía y Competitividad of Spain, Adenonet BIO2015-68990-REDT from the Ministerio de Economía y Competitividad of Spain, Red ADVANCE(CAT) project COMRDI15-1-0013 from Ris3CAT, and 2014SGR364 research grant from the 'Generalitat de Catalunya,' and cofunded by the European Regional Development Fund, a way to Build Europe (all to R. Alemany).

The costs of publication of this article were defrayed in part by the payment of page charges. This article must therefore be hereby marked *advertisement* in accordance with 18 U.S.C. Section 1734 solely to indicate this fact.

Received April 27, 2018; revised August 16, 2018; accepted October 10, 2018; published first October 15, 2018.

References

1. Uchibori R, Tsukahara T, Ohmine K, Ozawa K. Cancer gene therapy using mesenchymal stem cells. Int J Hematol 2014;99:377–82.
2. Najar M, Raicevic G, Crompot E, Fayyad-Kazan H, Bron D, Toungouz M, et al. The immunomodulatory potential of mesenchymal stromal cells: a story of a regulatory network. J Immunother 2016;39:45–59.
3. Garcia-Castro J, Alemany R, Cascallo M, Martinez-Quintanilla J, Arriero Mdel M, Lassaletta A, et al. Treatment of metastatic neuroblastoma with systemic oncolytic virotherapy delivered by autologous mesenchymal stem cells: an exploratory study. Cancer Gene Ther 2010;17:476–83.
4. Melen GJ, Franco-Luzon L, Ruano D, Gonzalez-Murillo A, Alfranca A, Casco F, et al. Influence of carrier cells on the clinical outcome of children with neuroblastoma treated with high dose of oncolytic adenovirus delivered in mesenchymal stem cells. Cancer Lett 2016;371:161–70.
5. Cejalvo T, Perise-Barrios AJ, Portillo ID, Laborda E, Rodriguez-Milla MA, Cubillo I, et al. Remission of spontaneous canine tumors after systemic cellular viroimmunotherapy. Cancer Res 2018;78:4891–4901.
6. Gebler A, Zabel O, Seliger B. The immunomodulatory capacity of mesenchymal stem cells. Trends Mol Med 2012;18:128–34.

7. Najar M, Raicevic G, Fayyad-Kazan H, Bron D, Toungouz M, Lagneaux L. Mesenchymal stromal cells and immunomodulation: a gathering of regulatory immune cells. Cytotherapy 2016;18:160–71.
8. Bunnell BA, Betancourt AM, Sullivan DE. New concepts on the immune modulation mediated by mesenchymal stem cells. Stem Cell Res Ther 2010;1:34.
9. Waterman RS, Tomchuck SL, Henkle SL, Betancourt AM. A new mesenchymal stem cell (MSC) paradigm: polarization into a pro-inflammatory MSC1 or an immunosuppressive MSC2 phenotype. PLoS One 2010;5: e10088.
10. Waterman RS, Henkle SL, Betancourt AM. Mesenchymal stem cell 1 (MSC1)-based therapy attenuates tumor growth whereas MSC2-treatment promotes tumor growth and metastasis. PLoS One 2012;7:e45590.
11. Najar M, Krayem M, Meuleman N, Bron D, Lagneaux L. Mesenchymal stromal cells and toll-like receptor priming: a critical review. Immune Network 2017;17:89–102.
12. Sangiorgi B, Panepucci RA. Modulation of immunoregulatory properties of mesenchymal stromal cells by toll-like receptors: potential applications on GVHD. Stem Cells Int 2016;2016:9434250.
13. Eichholz K, Bru T, Tran TT, Fernandes P, Welles H, Mennechet FJ, et al. Immune-complexed adenovirus induce AIM2-mediated pyroptosis in human dendritic cells. PLoS Pathog 2016;12:e1005871.
14. Alfano AL, Nicola Candia A, Cuneo N, Guttlein LN, Soderini A, Rotondaro C, et al. Oncolytic adenovirus-loaded menstrual blood stem cells overcome the blockade of viral activity exerted by ovarian cancer ascites. Mol Ther Oncol 2017;6:31–44.
15. Hakkarainen T, Sarkioja M, Lehenkari P, Miettinen S, Ylikomi T, Suuronen R, et al. Human mesenchymal stem cells lack tumor tropism but enhance the antitumor activity of oncolytic adenoviruses in orthotopic lung and breast tumors. Hum Gene Ther 2007;18:627–41.
16. Kidd S, Caldwell L, Dietrich M, Samudio I, Spaeth EL, Watson K, et al. Mesenchymal stromal cells alone or expressing interferon-beta suppress pancreatic tumors *in vivo*, an effect countered by anti-inflammatory treatment. Cytotherapy 2010;12:615–25.
17. Rincon E, Cejalvo T, Kanojia D, Alfranca A, Rodriguez-Milla MA, Gil Hoyos RA, et al. Mesenchymal stem cell carriers enhance antitumor efficacy of oncolytic adenoviruses in an immunocompetent mouse model. Oncotarget 2017;8:45415–31.
18. Yuan X, Zhang Q, Li Z, Zhang X, Bao S, Fan D, et al. Mesenchymal stem cells deliver and release conditionally replicative adenovirus depending on hepatic differentiation to eliminate hepatocellular carcinoma cells specifically. Cancer Lett 2016;381:85–95.
19. Moreno R, Rojas LA, Villellas FV, Soriano VC, Garcia-Castro J, Fajardo CA, et al. Human menstrual blood-derived mesenchymal stem cells as potential cell carriers for oncolytic adenovirus. Stem Cells Int 2017;2017:3615729.
20. Rojas JJ, Guedan S, Searle PF, Martinez-Quintanilla J, Gil-Hoyos R, Alcayaga-Miranda F, et al. Minimal RB-responsive E1A promoter modification to attain potency, selectivity, and transgene-arming capacity in oncolytic adenoviruses. Mol Ther 2010;18:1960–71.
21. Appledorn DM, Patial S, McBride A, Godbehere S, Van Rooijen N, Parameswaran N, et al. Adenovirus vector-induced innate inflammatory mediators, MAPK signaling, as well as adaptive immune responses are dependent upon both TLR2 and TLR9 *in vivo*. J Immunol 2008;181: 2134–44.
22. Cerullo V, Seiler MP, Mane V, Brunetti-Pierri N, Clarke C, Bertin TK, et al. Toll-like receptor 9 triggers an innate immune response to helper-dependent adenoviral vectors. Mol Ther 2007;15:378–85.
23. Wilson AA, Kwok LW, Porter EL, Payne JG, McElroy GS, Ohle SJ, et al. Lentiviral delivery of RNAi for *in vivo* lineage-specific modulation of gene expression in mouse lung macrophages. Mol Ther 2013;21:825–33.
24. Fajardo CA, Guedan S, Rojas LA, Moreno R, Arias-Badia M, de Sostoa J, et al. Oncolytic adenoviral delivery of an EGFR-targeting T-cell engager improves antitumor efficacy. Cancer Res 2017;77:2052–63.
25. Tanoue K, Rosewell Shaw A, Watanabe N, Porter C, Rana B, Gottschalk S, et al. Armed oncolytic adenovirus-expressing PD-L1 mini-body enhances antitumor effects of chimeric antigen receptor T cells in solid tumors. Cancer Res 2017;77:2040–51.
26. Calandra T, Roger T. Macrophage migration inhibitory factor: a regulator of innate immunity. Nat Rev Immunol 2003;3:791–800.
27. Romieu-Mourez R, Francois M, Boivin MN, Bouchentouf M, Spaner DE, Galipeau J. Cytokine modulation of TLR expression and activation in mesenchymal stromal cells leads to a proinflammatory phenotype. J Immunol 2009;182:7963–73.
28. Gupta KK, Xu Z, Castellino FJ, Ploplis VA. Plasminogen activator inhibitor-1 stimulates macrophage activation through Toll-like Receptor-4. Biochem Biophys Res Commun 2016;477:503–8.
29. Teigler JE, Kagan JC, Barouch DH. Late endosomal trafficking of alternative serotype adenovirus vaccine vectors augments antiviral innate immunity. J Virol 2014;88:10354–63.
30. Zhu J, Huang X, Yang Y. Innate immune response to adenoviral vectors is mediated by both Toll-like receptor-dependent and -independent pathways. J Virol 2007;81:3170–80.
31. Liu Q, Muruve DA. Molecular basis of the inflammatory response to adenovirus vectors. Gene Ther 2003;10:935–40.
32. Lyakh LA, Koski GK, Young HA, Spence SE, Cohen PA, Rice NR. Adenovirus type 5 vectors induce dendritic cell differentiation in human CD14(+) monocytes cultured under serum-free conditions. Blood 2002;99:600–8.
33. Ribas A, Dummer R, Puzanov I, VanderWalde A, Andtbacka RHI, Michielin O, et al. Oncolytic virotherapy promotes intratumoral T cell infiltration and improves anti-PD-1 immunotherapy. Cell 2017;170:1109–19.
34. Woller N, Gurlevik E, Fleischmann-Mundt B, Schumacher A, Knocke S, Kloos AM, et al. Viral infection of tumors overcomes resistance to PD-1-immunotherapy by broadening neoantigenome-directed T-cell responses. Mol Ther 2015;23:1630–40.
35. Parrish C, Scott GB, Migneco G, Scott KJ, Steele LP, Ilett E, et al. Oncolytic reovirus enhances rituximab-mediated antibody-dependent cellular cytotoxicity against chronic lymphocytic leukaemia. Leukemia 2015;29: 1799–810.
36. Cascallo M, Alonso MM, Rojas JJ, Perez-Gimenez A, Fueyo J, Alemany R. Systemic toxicity-efficacy profile of ICOVIR-5, a potent and selective oncolytic adenovirus based on the pRB pathway. Mol Ther 2007;15: 1607–15.
37. Kasono K, Blackwell JL, Douglas JT, Dmitriev I, Strong TV, Reynolds P, et al. Selective gene delivery to head and neck cancer cells via an integrin targeted adenoviral vector. Clin Cancer Res 1999;5:2571–9.
38. Lee AJ, Chen B, Chew MV, Barra NG, Shenouda MM, Nham T, et al. Inflammatory monocytes require type I interferon receptor signaling to activate NK cells via IL-18 during a mucosal viral infection. J Exp Med 2017;214:1153–67.
39. Michel T, Hentges F, Zimmer J. Consequences of the crosstalk between monocytes/macrophages and natural killer cells. Front Immunol 2012;3: 403.
40. Gasteiger G, Rudensky AY. Interactions between innate and adaptive lymphocytes. Nat Rev Immunol 2014;14:631–9.
41. Alcayaga-Miranda F, Cuenca J, Luz-Crawford P, Aguila-Diaz C, Fernandez A, Figueroa FE, et al. Characterization of menstrual stem cells: angiogenic effect, migration and hematopoietic stem cell support in comparison with bone marrow mesenchymal stem cells. Stem Cell Res Ther 2015;6:32.
42. Darzi S, Werkmeister JA, Deane JA, Gargett CE. Identification and characterization of human endometrial mesenchymal stem/stromal cells and their potential for cellular therapy. Stem Cells Translat Med 2016;5: 1127–32.
43. Rodrigues MC, Lippert T, Nguyen H, Kaelber S, Sanberg PR, Borlongan CV. Menstrual blood-derived stem cells: *in vitro* and *in vivo* characterization of functional effects. Adv Exp Med Biol 2016;951:111–21.
44. Rodriguez-Garcia A, Gimenez-Alejandre M, Rojas JJ, Moreno R, Bazan-Peregrino M, Cascallo M, et al. Safety and efficacy of VCN-01, an oncolytic adenovirus combining fiber HSG-binding domain replacement with RGD and hyaluronidase expression. Clin Cancer Res 2015;21:1406–18.
45. Eriksson E, Milenova I, Wenthe J, Stahle M, Leja-Jarblad J, Ullenhag G, et al. Shaping the tumor stroma and sparking immune activation by CD40 and 4–1BB signaling induced by an armed oncolytic virus. Clin Cancer Res 2017;23:5846–57.
46. Tahtinen S, Blattner C, Vaha-Koskela M, Saha D, Siurala M, Parviainen S, et al. T-cell therapy enabling adenoviruses coding for IL2 and TNFalpha induce systemic immunomodulation in mice with spontaneous melanoma. J Immunother 2016;39:343–54.